Hindawi
Evidence-Based Complementary and Alternative Medicine
Volume 2022, Article ID 4172531, 18 pages
https://doi.org/10.1155/2022/4172531

Research Article

Comprehensive Computational Analysis of Honokiol Targets for Cell Cycle Inhibition and Immunotherapy in Metastatic Breast Cancer Stem Cells

Skolastika Skolastika,[1] **Naufa Hanif**,[2] **Muthi Ikawati**,[1,2] **and Adam Hermawan**[1,2]

[1]*Laboratory of Macromolecular Engineering, Department of Pharmaceutical Chemistry, Faculty of Pharmacy, Universitas Gadjah Mada Sekip Utara II, 55281 Yogyakarta, Indonesia*
[2]*Cancer Chemoprevention Research Center, Faculty of Pharmacy, Universitas Gadjah Mada Sekip Utara II, 55281 Yogyakarta, Indonesia*

Correspondence should be addressed to Adam Hermawan; adam_apt@ugm.ac.id

Received 19 January 2022; Accepted 12 April 2022; Published 8 July 2022

Academic Editor: Zhaohui Liang

Breast cancer stem cells (BCSCs) play a critical role in chemoresistance, metastasis, and poor prognosis of breast cancer. BCSCs are mostly dormant, and therefore, activating them and modulating the cell cycle are important for successful therapy against BCSCs. The tumor microenvironment (TME) promotes BCSC survival and cancer progression, and targeting the TME can aid in successful immunotherapy. Honokiol (HNK), a bioactive polyphenol isolated from the bark and seed pods of *Magnolia spp*., is known to exert anticancer effects, such as inducing cell cycle arrest, inhibiting metastasis, and overcoming immunotherapy resistance in breast cancer cells. However, the molecular mechanisms of action of HNK in BCSCs, as well as its effects on the cell cycle, remain unclear. This study aimed to explore the potential targets and molecular mechanisms of HNK on metastatic BCSC (mBCSC)-cell cycle arrest and the impact of the TME. Using bioinformatics analyses, we predicted HNK protein targets from several databases and retrieved the genes differentially expressed in mBCSCs from the GEO database. The intersection between the differentially expressed genes (DEGs) and the HNK-targets was determined using a Venn diagram, and the results were analyzed using a protein-protein interaction network, hub gene selection, gene ontology and Kyoto Encyclopedia of Genes and Genomes pathway enrichment analyses, genetic alteration analysis, survival rate, and immune cell infiltration levels. Finally, the interaction between HNK and two HNK-targets regulating the cell cycle was analyzed using molecular docking analysis. The identified potential therapeutic targets of HNK (PTTH) included *CCND1*, *SIRT2*, *AURKB*, *VEGFA*, *HDAC1*, *CASP9*, *HSP90AA1*, and *HSP90AB1*, which can potentially inhibit the cell cycle of mBCSCs. Moreover, our results showed that PTTH could modulate the PI3K/Akt/mTOR and HIF1/NFkB/pathways. Overall, these findings highlight the potential of HNK as an immunotherapeutic agent for mBCSCs by modulating the tumor immune environment.

1. Introduction

Breast cancer was the most prevalent cancer in 2020 (in terms of new cases) and the leading cause of cancer-related deaths among females [1]. According to the World Health Organization, breast cancer has the highest incidence rate in Indonesia, with a mortality rate of 22,692 cases per year [1]. By 2040, the incidence is predicted to reach 89,512 cases [1]. Chemotherapy, along with surgery, radiation, and mastectomy, is the most common treatment [2]. Chemoresistance, or the insensitivity of cancer cells to drug therapy, is a major factor in the failure of chemotherapy against breast cancer.

Breast cancer stem cells (BCSCs) are one of the main factors driving chemoresistance, thereby contributing to poor prognosis and clinical outcomes [3–5]. BCSCs can develop into many cell types and repopulate heterogeneous tumors following conventional chemotherapy or

radiotherapy [4, 6]. BCSCs are mostly dormant and therefore activating dormant cells, and modulating the cell cycle is important for achieving successful BCSCs therapy [7]. Recurrent tumors are highly aggressive, potentially cross-drug resistant, highly metastatic, and have a poor prognosis. A previous study demonstrated that immune cells such as CD8+ lymphocytes induce epithelial to mesenchymal transition of BCSCs [8] Moreover, the tumor microenvironment (TME) promotes BCSC survival and cancer progression [9], and hence it can prevent the success of immunotherapy [10] The use of combination therapy, in which both chemotherapy and natural compounds are used to target metastatic BCSCs (mBCSCs), could be a successful approach to overcome chemoresistance and achieve clinical success in treating breast cancer.

Honokiol (HNK; 3,5-di-(2-propenyl)-1,1′-biphenyl-2,2′-diol, Figure 1(a)) is a bioactive polyphenol isolated from the bark and seed pods of *Magnolia spp*., that is widely used in traditional Asian medicine [11]. HNK controls various intracellular signaling pathways involved in cancer, including those related to nuclear factor kappa B (NF-κB), signal transducers and activators of transcription 3 (STAT3), epidermal growth factor receptor (EGFR), and mammalian targets of rapamycin (mTOR) [12]. HNK-mediated cell cycle arrest is achieved via the downregulation of cyclin D1, an inhibition of cyclin E1, cyclin-dependent kinase 2, cyclin-dependent kinase 4, cMYC, and RB, CSK/EGFR signaling, and the upregulation of p27 and p21 [13, 14]. HNK has shown to inhibit matrix metalloproteinases, thereby reducing cell migration, invasion, and metastasis, while also regulating VEGFR signally, exerting an anti-angiogenic effect [15, 16]. In addition, HNK has been reported to successfully inhibit the pluripotency factors POU5F1, Nanog, and SOX2, and to abolish the BCSC-like phenotype [17–20] (p11). Moreover, HNK decreases drug resistance by inhibiting P-gp regulation and by enhancing apoptosis [21]. In addition, HNK also inhibits the PI3K/mTOR pathway, contributing to circumventing immunotherapeutic resistance in glioma and breast cancer cells [22]. Even though increasing research has evaluated the effects of HNK in the cell cycle, BCSCs, and metastasis, the molecular mechanisms underlying its effects on metastatic BCSC cell cycle axis and immunotherapy have not been elucidated.

This study aimed to explore the molecular mechanisms underlying HNK-mediated mBCSC-cell cycle arrest, as well as to assess the impact of this compound on the immune environment using bioinformatics studies.

2. Materials and Methods

2.1. Data Collection and Differentially Expressed Genes' (DEGs) Identification. Proteins that interact with HNK were searched using STITCH (https://stitch.embl.de), [23]. Swisstargetprediction (https://www.swisstargetprediction.ch), [24] canSAR Black (https://cansarblack.icr.ac.uk/) [25], and SEA (https://sea.bkslab.org/) [26]. The retrieved proteins were considered as HNK-mediated proteins (HMPs) and were included in the subsequent analyses. The microarray data of metastatic breast cancer stem cells were collected from the GEO database (https://www.ncbi.nlm.nih.gov/geo) using keywords such as metastatic breast cancer stem cells, and *Homo sapiens*. The inclusion criteria were: use of patient samples or patient-derived xenografts; focus on metastatic breast cancer; characterization of breast cancer stem cells; and clear description of the identity of samples in the GSE datasets. The exclusion criteria included: use of breast cancer cell lines; no emphasis on metastatic breast cancer; no characterization of breast cancer stem cells; and ambiguity around the identity of samples in the GSE datasets. One GSE Dataset (GSE151191) was selected among the 62 datasets for this study (Supplementary Figure 1). GEO2R, a web-based interactive program (https://www.ncbi.nlm.nih.gov/geo/geo2r) that compares two groups of samples under the same conditions, was used to identify the DEGs between primary and metastatic tumors, on the basis of the following criteria for significance: $P < 0.05$ and log | Fold Change| > 1. Using [27], the overlapping proteins between the HMP and those encoded by the DEGs were identified and further analyzed using a protein-protein interaction (PPI) network.

2.2. Construction of the PPI Network. The PPI was constructed and displayed using STRING-DB v11.0 and Cytoscape software, respectively [28, 29]. Proteins included in the top-10 rank according to the Maximal Clique Centrality (MCC) score determined by the Cyto-Hubba plugin were considered hub genes [30].

The hub genes were subjected to GO and KEGG enrichment analyses using the tools [31] and WebGestalt [32]. Statistical significance was set at $P < 0.05$.

2.3. Genetic Alterations Analysis. The proteins nominated by GO and KEGG enrichment analyses and an in-depth literature study on the hub genes were used to determine the potential therapeutic targets of HNK (PTTH). In this study, genes encoding PTTH such as *CCND1*, *SIRT2*, *AURKB*, *VEGFA*, *HDAC1*, *CASP9*, *HSP90AA1*, and *HSP90AB1* were screened for genetic changes in all breast cancer studies available in the cBio-portal database ((https://www.cbioportal.org) [33]. The studies with the highest number of genetic changes were selected for analysis further connectivity.

2.4. Survival Rate and Immune Cell Infiltration Level. The online database Gene Expression Profiling Interactive Analysis (GEPIA, https://gepia.cancer-pku.cn) was utilized to analyze the contribution of PTTH to the overall survival (OS) [34]. Tumor Immune Estimation Resource (TIMER) (https://cistrome.shinyapps.io/timer/) was used to analyze the correlation between PTTH expression levels and immune cell infiltration level [35].

2.5. Validation of the mRNA and Protein Expression Levels of PTTH. The mRNA and protein expression levels of PTTH were determined using TNMPlot and Human Protein Atlas

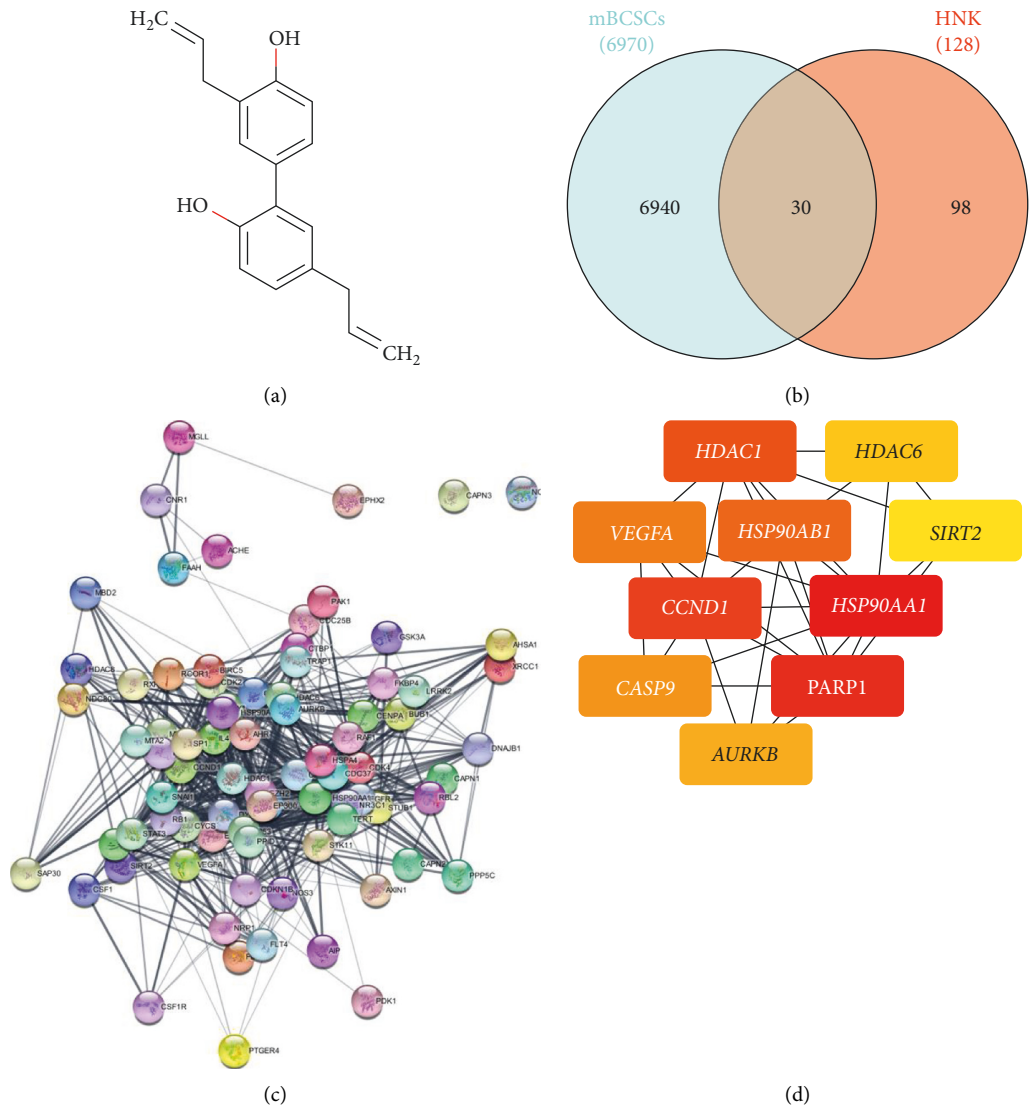

FIGURE 1: (a) Structure of honokiol. (b) Venn diagram of potential therapeutic targets of honokiol (PTTH) in breast cancer stem cells (BCSCs). (c) Protein-protein interaction (PPI) network of honokiol and the interacting proteins. (d) Top-10 hub genes determined according to the Maximal Clique Centrality (MCC) score.

(HPA). Differentially expressed genes and mRNA levels in tumor, normal, and metastatic tissues were analyzed using TNMplot (https://www.tnmplot.com/) [36], in which the database utilized data from GEO or RNA-seq libraries from The Cancer Genome Atlas (TCGA), Therapeutically Applicable Research to Generate Effective Treatments (TARGET), and The Genotype-Tissue Expression (GTEx). The protein expression levels were analyzed using the Human Protein Atlas (HPA) (https://www.proteinatlas.org/) [37], an online database that contains a wide range of transcriptomic and proteomic data from various tissues and cells.

2.6. Molecular Docking. To predict the binding properties of HNK to AURKB and RAC-1 through molecular docking, computational prediction was conducted on a Windows 10 operating system, Intel Core (TM) i5-10th Gen with 8 GB of RAM. MOE 2010 (licensed from Faculty of Pharmacy UGM) was used for docking simulation, RMSD-docking score calculation, and visualization interaction. The PDB IDs of the proteins AURKB and RAC-1 (3ZCW and 3TH5, respectively) were searched for in https://rcsb.org. The HNK structure was obtained from PubChem, subjected to conformational search, and minimized in the MOE using Energy Minimize Menu. For the docking simulation setting, London dG was used for both Rescoring 1 and Rescoring 2. Triangle Matcher was used for score function and placement setting, and Forcefield was used to refine the docking results from 30 retained settings. The results of this method will determine which conformation has the lowest binding interaction between the ligand and its receptor.

3. Results

3.1. DEG and HMP Identification. The DEGs are considered to be the molecular drivers and/or molecular biomarkers of

various phenotypes [38]. The identification of DEGs was carried out to determine the genes that act as biomolecular markers of metastatic breast cancer stem cells (mBCSCs). In total, 6,970 DEGs in the GSE 151191 dataset were found to be up/downregulated in metastatic breast cancer stem cells, according to the adjusted P value of <0.05, and a $|\log FC| \geq 1.0$ (Supplementary Table 1). Subsequently, proteins that interact directly and/or indirectly with HNK, referred to as HMPs, were identified. A total of 128 HMPs were retrieved from Swisstargetprediction, STITCH, canSAR Black, and SEA (Supplementary Table 2). Finally, 30 overlapping genes (OGs), including 18 upregulated and 12 downregulated genes, were identified to be both HMP and DEGs (Figure 1(b); Table 1).

3.2. PPI Network. To deepen our understanding of the interactions between the 30 OGs, we constructed a PPI network. The network contained 40 nodes and 134 edges, with an average node degree of 6.7, an average local clustering coefficient of 0.618, and a PPI enrichment value < 1.0e-16 (Figure 1(c)). Further analysis identified hub genes within the PPI network (Figure 1(d)), which included NAD-dependent deacetylase sirtuin 2 (SIRT2), cyclin D1 (CCND1), serine/threonine-protein kinase Aurora-B (AURKB), vascular endothelial growth factor A (VEGFA), histone deacetylase 1 (HDAC1), caspase 9 (CASP9), heat shock protein HSP 90-alpha (HSP90AA1), and heat shock protein HSP 90-beta (HSP90AB1) (Table 2).

3.3. GO and KEGG Pathway Enrichment Analysis. The functions of the OGs were further investigated using GO and KEGG pathway enrichment analyses. The biological processes in which these OGs were implicated are summarized in Figure 2(a). Among the identified biological processes, cell communication, metabolic process, cellular component organization, multicellular organismal process, developmental process, response to stimulus, and biological regulation are strongly linked to cancer progression. According to the enrichment analysis of cellular components, the OGs were abundant in the nucleus, cytosol, membrane-enclosed lumen, and protein-containing complex (Figure 2(a)). Finally, the OGs were enriched in the molecular function protein binding (Figure 2(a)). KEGG pathway enrichment analysis demonstrated that the OGs were particularly enriched in the PI3K-Akt signaling pathway, pathways associated with cancer, and the regulation of the cell cycle (Supplementary Table 3).

3.4. Genetics Alteration Analysis. Eight genes (*SIRT2*, *CCND1*, *AURKB*, *VEGFA*, *HDAC1*, *CASP9*, *HSP90AA1*, and *HSP90AB1*) that play an essential role in the growth and development of mBCSC were selected from hub genes and referred to as potential therapeutic targets of honokiol (PTTH). Genetic variation within these genes was analyzed using cBioportal. The breast cancer study with the highest number of genetic changes was selected for further analysis (Figure 2(b)). Oncoprint was used to determine the percentage of PTTH gene alterations in patients with mBC. Genetic alterations in PTTH ranged from 1.1% to 35% in the 180 patient samples analyzed (Figure 2(c)), with amplification being the most common gene alteration. The genes that were most frequently mutated were *CCND1* (35%), *HSP90AB1* (11%), and *VEGFA* (8%). Mutual exclusivity analysis showed that *VEGFA* mutations significantly co-occurred with *HSP90AB1* mutations (Table 3). Copy number alterations (CNAs) are particularly common in cancer and play a significant role in its development and progression. CNA status can be homozygously deleted (shallow deletion), heterozygously deleted (deep deletion), diploid, gained (amplification event with relatively few copies), or amplified (amplification event with many copies). CNAs analysis revealed that *SIRT2* mRNA expression was lower in shallow deletion cases and higher in amplification cases than in diploids (normal/without change) (Figure 2(d)). *HDAC1* and *HSP90AB1* mRNA expression was lower in cases with shallow deletions and higher in cases with gain. *HSP90AA1* mRNA expression was lower in patients with gain than in those with diploid gain. *CASP9* mRNA expression was lower in the gain than in the in shallow deletion cases, but not significantly different from that in diploid cases. All CNAs other than those mentioned were not differently expressed. Finally, the cBioportal pathway analysis showed that the cell cycle pathway is the main pathway that is disrupted by PTTH genetic alterations. Among the genes involved in the regulation of cell pathway, *CCND1*, encoding cyclin D1, was identified as PTTH (Figure 2(e)).

3.5. Survival Rate and Immune Cell Infiltration Level. To assess the clinical value of PTTH genes' expression levels, we examined whether they are associated with the OS or prognosis of patients with breast cancer. Low expression levels of *CASP9* and *HSP90AB1* were significantly associated with poor OS ($P < 0.05$) (Figure 3(a)). To understand the role of the immune microenvironment in the development and prognosis of patients with BRCA mutations, we analyzed the correlation between the expression levels of PTTH and immunocyte infiltration. The expression level of PTTH was either positively or negatively related to the infiltration level of different immune cells, indicating that PTTH modulated the immunologic microenvironment by influencing immune cell infiltration. The expression levels of *CCND1*, *VEGFA*, *AURKB*, *HDAC1*, *HSP90AA1*, and *HSP90AB1* were positively correlated with immune cell infiltration levels, whereas the expression levels of *SIRT2* and *CASP9* were negatively correlated with the tumor purity of BRCA (Figure 3(b)). Additionally, the B cells' infiltration level was positively correlated with the expression levels of *HSP90AB1* and *AURKB*, and negatively correlated with the expression level of *CCND1*. Moreover, we observed a positive correlation between CD8+ T cells' infiltration levels and *SIRT2*, *HDAC1*, *CASP9*, and *HSP90AA1* expression levels, and between CD4+ T cells' infiltration levels and *SIRT2*, *HDAC1*, and *CASP9* expression levels. However, CD4+ T cells' infiltration levels were negatively correlated with

Table 1: Potential therapeutic targets of honokiol (PTTH) in metastatic breast cancer stem cells (mBCSCs).

No.	Protein symbol	Protein name	Database
1	*CASP9*	Caspase 9	STITCH
2	IL4	Interleukin 4	STITCH
3	PDK1	Pyruvate dehydrogenase kinase isoform 1	Swisstargetprediction
4	*CCND1*	Cyclin D1	STITCH
5	CSF1R	Macrophage colony stimulating factor receptor	Swisstargetprediction
6	TRAP1	Heat shock protein 75 kDa, mitochondrial	Swisstargetprediction
7	VEGFA	Vascular endothelial growth factor A	STITCH
8	HDAC8	Histone deacetylase 8	Swisstargetprediction
9	CAPN1	Calpain 1	STITCH
10	PARP1	Poly (ADP-ribose) polymerase-1	Swisstargetprediction
11	MGLL	Monoglyceride lipase	Swisstargetprediction
12	NQO2	Quinone reductase 2	Swisstargetprediction
13	RXRA	Retinoid X receptor alpha	canSAR Black
14	CNR1	Cannabinoid receptor 1	Swisstargetprediction
15	*HSP90AB1*	Heat shock protein HSP 90-beta	Swisstargetprediction
16	AURKB	Serine/threonine-protein kinase Aurora-B	Swisstargetprediction
17	PTGER4	Prostanoid EP4 receptor	Swisstargetprediction
18	*HSP90AA1*	Heat shock protein HSP 90-alpha	Swisstargetprediction
19	DYRK1A	Dual-specificity tyrosine-phosphorylation regulated kinase 1A	Swisstargetprediction
20	GSK3A	Glycogen synthase kinase-3 alpha	Swisstargetprediction
21	ACHE	Acetylcholinesterase	Swisstargetprediction
22	PAK1	Serine/threonine-protein kinase PAK 1	Swisstargetprediction
23	FAAH	Anandamide amidohydrolase	Swisstargetprediction
24	CAPN2	Calpain 2	STITCH
25	CAPN3	Calpain 3	STITCH
26	*HDAC1*	Histone deacetylase 1	Swisstargetprediction
27	EPHX2	Epoxide hydratase	Swisstargetprediction
28	CDC25B	Dual specificity phosphatase Cdc25B	Swisstargetprediction
29	HDAC6	Histone deacetylase 6	Swisstargetprediction
30	SIRT2	NAD-dependent deacetylase sirtuin 2	Swisstargetprediction

Table 2: Top-10 hub genes by Maximal Clique Centrality (MCC) score, as analyzed by CytoHubba.

Rank	Gene symbol	MCC score
1	HSP90AA1	132
2	PARP1	102
3	*CCND1*	98
4	HDAC1	67
5	HSP90AB1	62
6	VEGFA	53
7	CASP9	28
8	AURKB	26
9	HDAC6	24
10	SIRT2	18

HSP90AA1 expression levels. Infiltration levels of macrophages were positively correlated with *CCND1*, *SIRT2*, *CASP9*, and *HSP90AA1* expression levels, whereas they were negatively correlated with *AURKB* expression levels. Neutrophil infiltration levels were positively correlated with *SIRT2*, *AURKB*, *VEGFA*, *HDAC1*, *CASP9*, *HSP90AA1*, and *HSP90AB1*. Dendritic cell infiltration levels were negatively correlated with *CCND1* expression levels and positively correlated with *SIRT2*, *AURKB*, and *HDAC1* expression levels. Other non-mentioned data are not statistically significant.

3.6. Validation of the mRNA Expression Level and the Protein Expression Level of PTTH. The expression levels of *CCND1*, *AURKB*, *HDAC1*, *VEGFA*, *HSP90AA1*, and *HSP90AB1* were increased in the BC tissue, and even higher in mBC (Figure 4(a)). *CASP9* expression levels were not significantly different between normal, tumor, and metastatic breast cancer tissues. Interestingly, *SIRT2* expression was decreased in breast cancer tissues, but increased in metastatic tissues compared to normal tissues. These results were supported by immunohistochemical data from HPA, that showed that CCND1, AURKB, and HDAC1 were overexpressed in the nucleus, while SIRT2, VEGFA, HSP90AA1, and HSP90AB1 were overexpressed in the cytoplasmic/membranous region (Figure 4(b)). Finally, CASP9 was not differentially expressed between the normal tissue and the tumor tissue.

3.7. Molecular Docking. Molecular docking analysis revealed that AURKB and RAC-1 could bind to their respective native ligands and to HNK (Figure 5). The affinity of the interaction between these proteins and HNK was similar to that of their natural ligands. The interaction between AURKB and its native ligand ADP was stronger than that between *AURKB* and HNK according to the docking score (–12.89 and–8.68, respectively, Table 4). Furthermore, ADP interacted with several amino acids of AURKB, such as

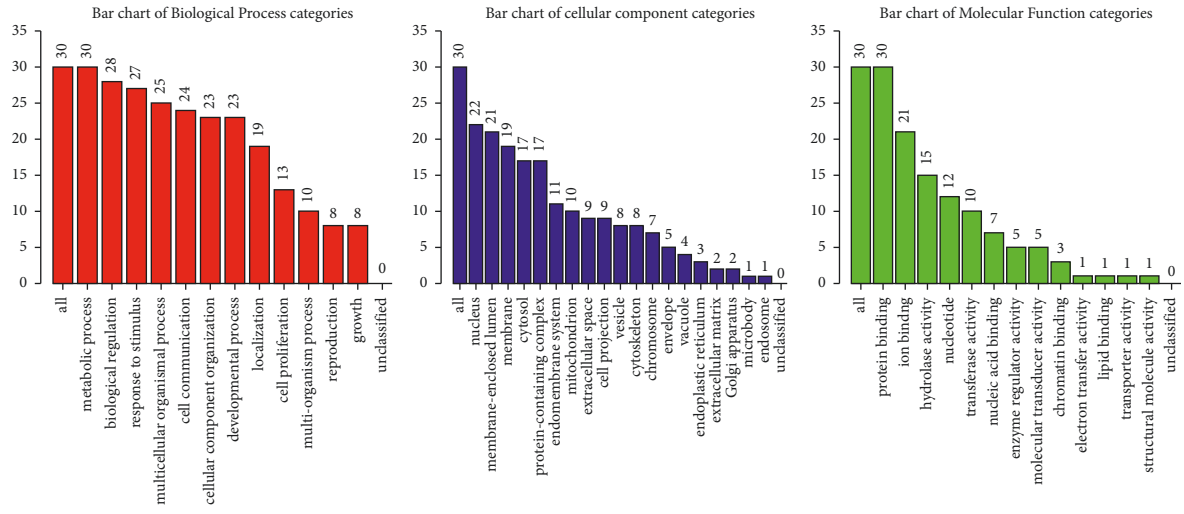

(a)

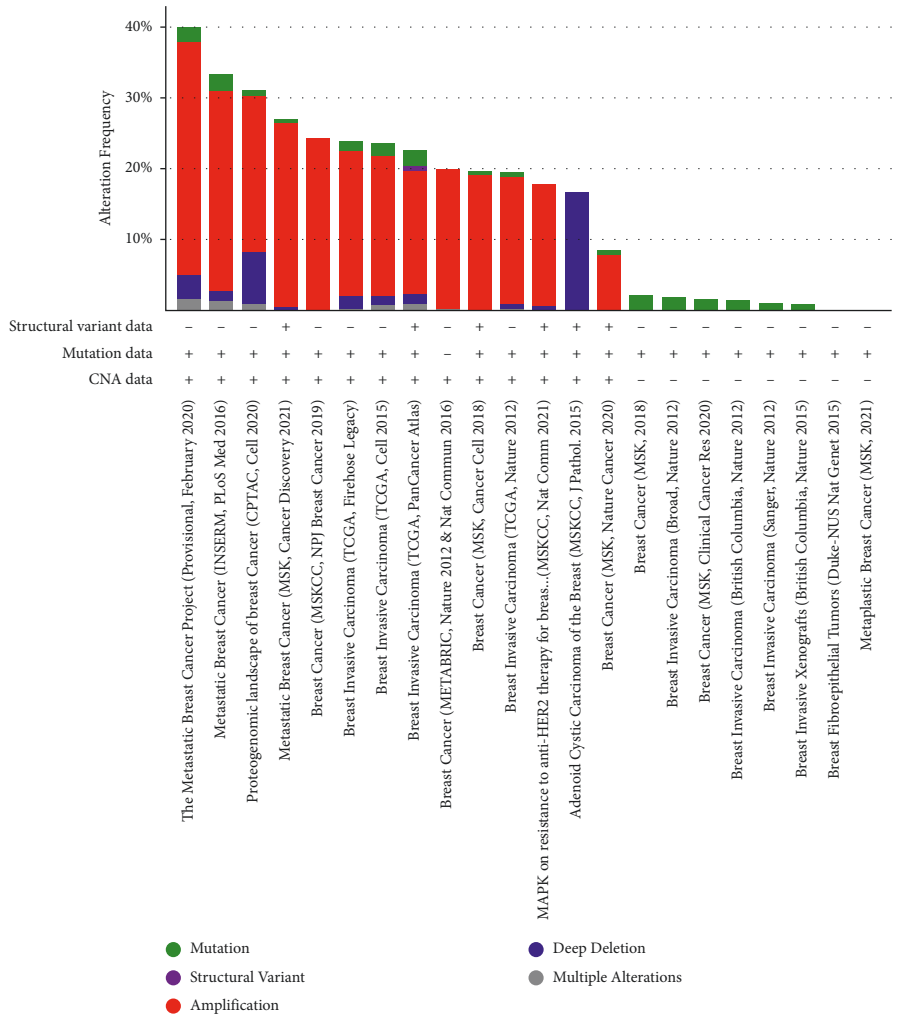

(b)

Figure 2: Continued.

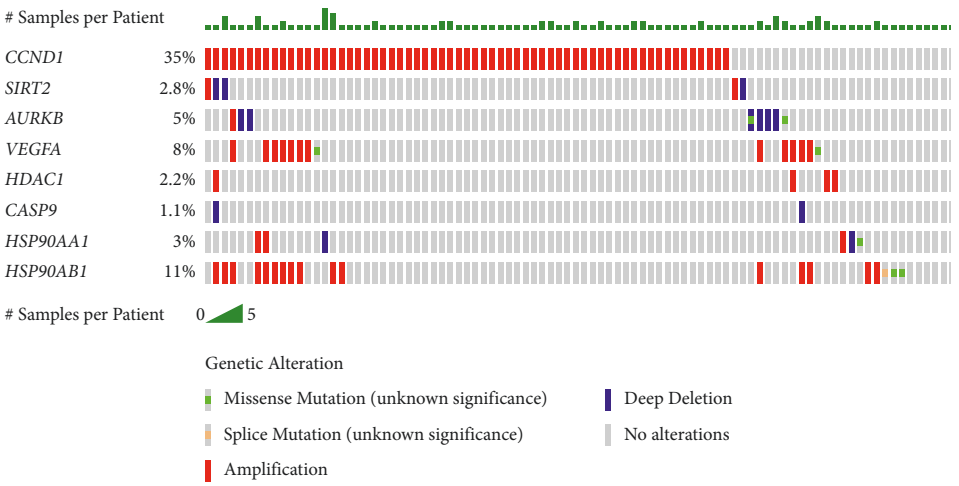

(c)

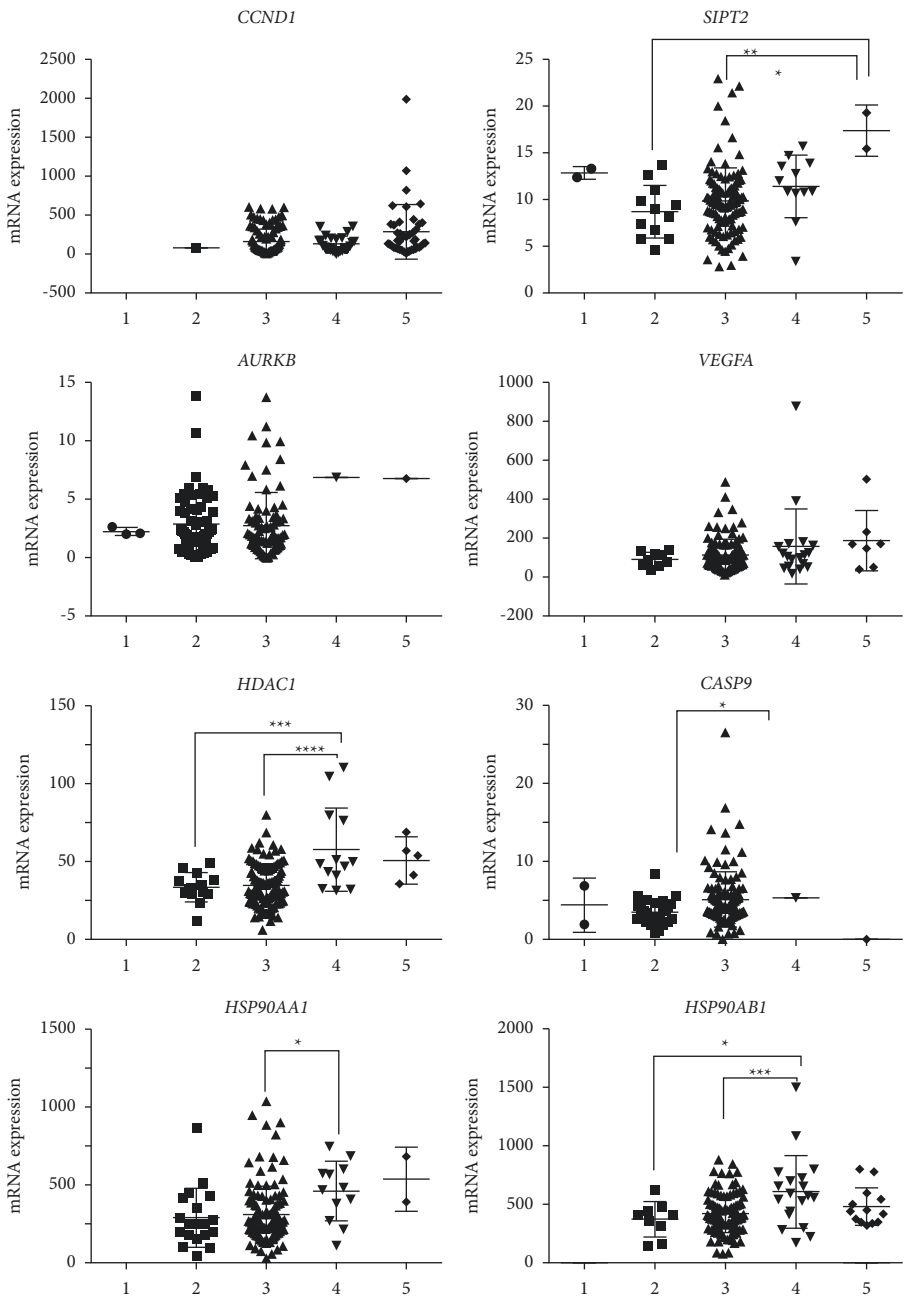

(d)

Figure 2: Continued.

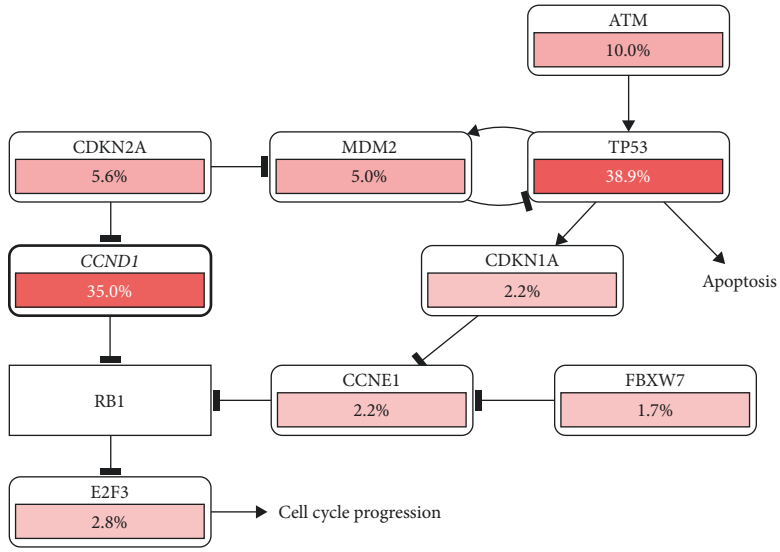

(e)

Figure 2: (a) Gene ontology (GO) analysis of potential therapeutic targets of honokiol (PTTH) results using WebGestalt. (b) Overview of genetic alterations in *CCND1, SIRT2, AURKB, VEGFA, HDAC1, CASP9, HSP90AA1*, and *HSP90AB1* based in samples from several breast cancer studies. (c) Oncoprint analysis of *CCND1, SIRT2, AURKB, VEGFA, HDAC1, CASP9, HSP90AA1*, and HSP90AB1 on The Metastatic Breast Cancer Project (Provisional, February 2020) dataset. (d) mRNA expression levels of *CCND1, SIRT2, AURKB, VEGFA, HDAC1, CASP9, HSP90AA1*, and *HSP90AB1* on the Metastatic Breast Cancer Project (Provisional, February 2020) as analyzed using cBioportal. 1: deep deletion, 2: shallow deletion, 3: diploid; 4: gain; 5: amplification. Statistical analyses were done by one-way ANOVA using Tukey's multiple comparison test. The symbol *or**or***or**** symbolizes $P < 0.05$ or $P < 0.01$ or $P < 0.001$ or $P < 0.001$, respectively. (e) Pathways related to genetic alterations predicted by cBioportal. The results showed that genetic alterations of the PTTH disrupted the pathways regulating the cell cycle.

Table 3: Mutual exclusivity analysis' results of the potential therapeutic targets of honokiol (PTTH).

A	B	Log2 odds ratio	*P* value	Tendency
HSP90AB1	*VEGFA*	>3	<0.001	Co-occurrence

Gly108, Gly110, Lys111, and Thr112, while HNK interacted with only one amino acid (Pro27). Likewise, the binding interaction between Rac-1 and its native ligand (phosphoaminophosphonic acid-guanylate ester/GNP; docking score −21.38) was stronger than that between Rac-1 and HNK (docking score −18.17). This was a result of the number of amino acids that the compounds interacted with and the distance between the interacting amino acids and the compound. For instance, the distance between Thr17 and GNP was much closer (1.82 Å) than that with HNK (3.35). However, despite the lower affinity of the interaction, HNK could potentially compete with the native ligands to inhibit the function of these proteins.

4. Discussion

This study identified eight PTTHs, including *CCND1*, *SIRT2*, *AURKB*, *VEGFA*, *HDAC1*, *CASP9*, *HSP90AA1*, and *HSP90AB1*. The expression levels of these genes were strongly associated with immune infiltration levels. The tumor microenvironment influences angiogenesis and the immune response, and has long been recognized as a primary determinant of long-term tumor progression [39–41]. In addition, it can greatly impact the effectiveness of immunotherapy, highlighting the need of its further understanding [42].

Cyclin D1, encoded by *CCND1*, is considered an oncogene that promotes cell proliferation, growth, angiogenesis, and resistance to chemotherapy and radiotherapy [43, 44]. In this study, we revealed that *CCND1* expression was positively correlated with BRCA purity and macrophage infiltration levels, and negatively correlated with B cell and dendritic cell infiltration levels. Many studies have shown that tumor-associated macrophages play an important role in the proliferation, invasion, angiogenesis, and metastasis of human breast carcinoma, and that increased macrophage tumor infiltration confers metastatic potential and is associated with poor prognosis in breast cancer [42]. Our findings are in line with those of Pestell et al., who demonstrated that cyclin D1 expression was increased in human cancer stroma, and promoted tumor inflammation, angiogenesis, and stem cell expansion in advanced breast cancer [41]. Interestingly, a previous study reported that HNK could inhibit cyclin D1 expression [14].

SIRT2, an NAD-dependent histone deacetylase, has been suggested to be a promising therapeutic target in cancer

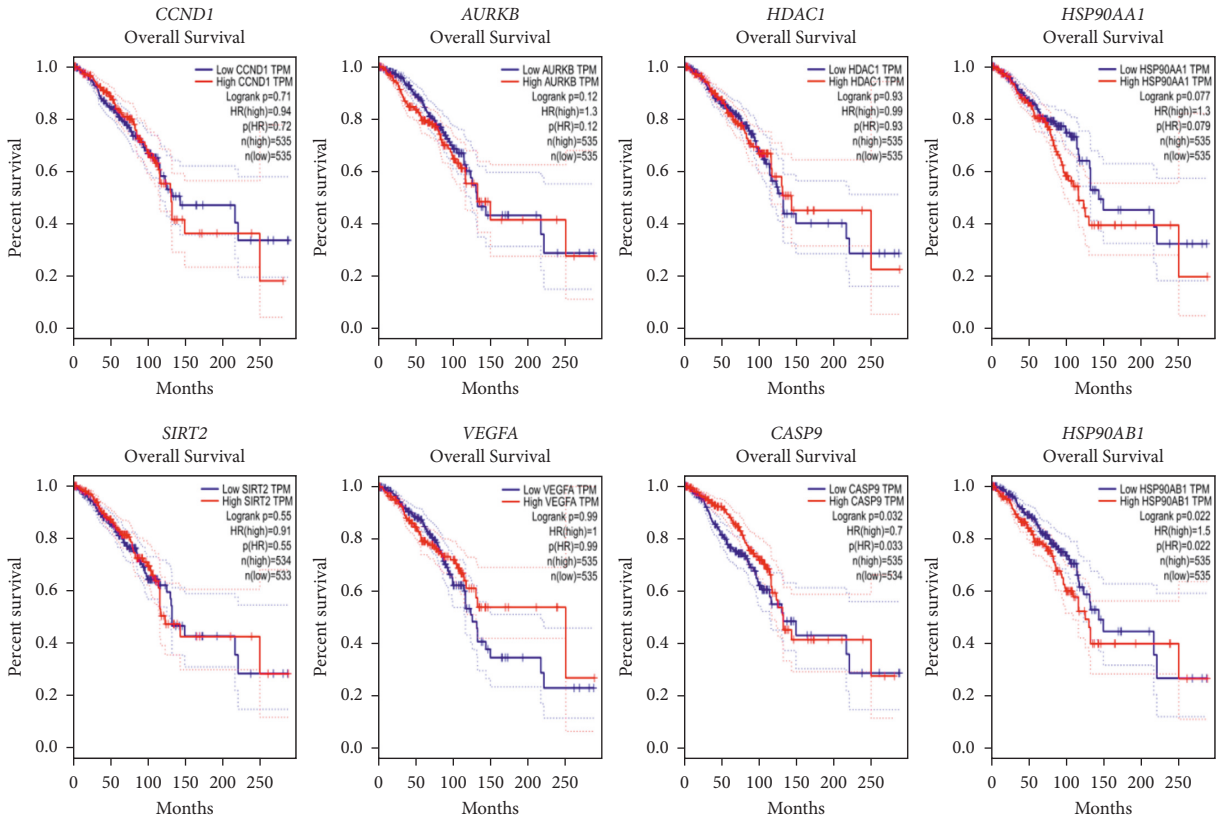

(a)

Figure 3: Continued.

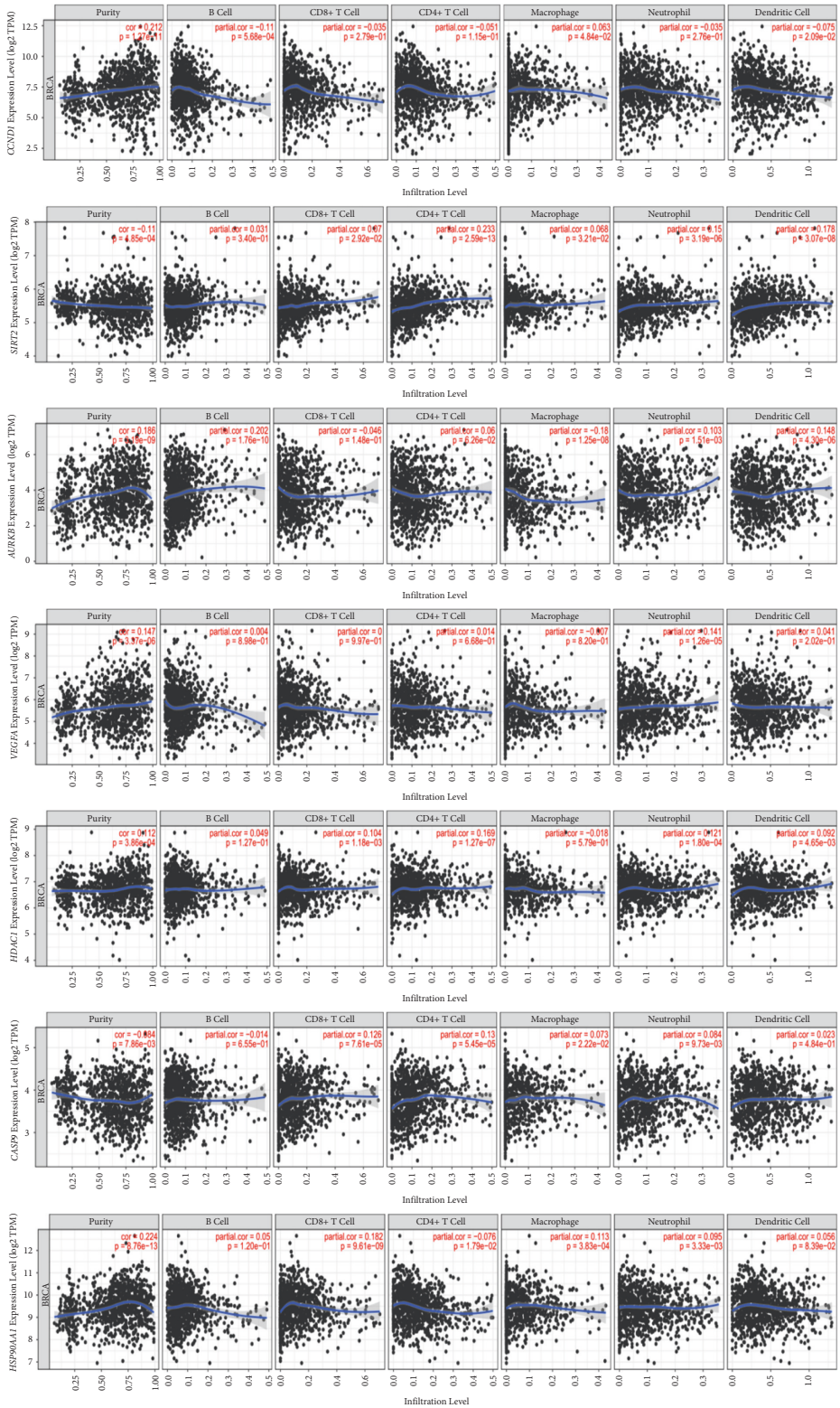

(b)

Figure 3: Continued.

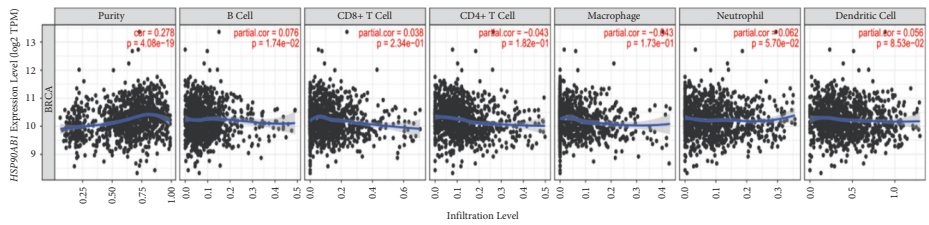

(c)

Figure 3: (a) Association between the expression levels of *CCND1, SIRT2, AURKB, VEGFA, HDAC1, CASP9, HSP90AA1*, and *HSP90AB1* and the overall survival in the breast cancer samples from The Cancer Genome Atlas. (b) Correlation analysis between the expression levels of *CCND1, SIRT2, AURKB, VEGFA, HDAC1, CASP9, HSP90AA1*, and *HSP90AB1* and the infiltration levels of B cells, CD8+ T cells, CD4+ T cells, macrophages, neutrophils, and dendritic cells.

treatment [47]. *SIRT2* is thought to affect carcinogenesis in a context-dependent manner, affecting epigenetic pathways implicated in cancer initiation, development, and progression [48–50]. *SIRT2* expression level was negatively correlated with BRCA purity, but positively correlated with CD8+ T cell, CD4+ T cell, macrophages, neutrophils, and dendritic cells' infiltration levels. These results confirm those of previous studies, in which *SIRT2* expression level and CD8+ T cell infiltration level were positively correlated in breast cancer patients [51]. In addition, systemic SIRT2 has been suggested to promote tumor development by suppressing NK cells [42]. Interestingly, *SIRT2* expression was significantly lower in breast cancer than in normal breast tissue, suggesting that *SIRT2* may act as a tumor suppressor during the initiation of tumorigenesis. Moreover, a previous study reported that high *SIRT2* expression in advanced tumor tissues is associated with poor prognosis, suggesting that *SIRT2* may function as an oncogene [50].

VEGFA is a cytokine that promotes vascular development and the formation of new blood vessels from preexisting vascular networks during embryogenesis [52–54]. In addition, VEGFA can also be released by cancer and stromal cells [55]. In several murine and human cancer models, it has been demonstrated that VEGFA stimulates the tumor-initiating epithelial–mesenchymal transition and metastasis, and that *VEGFA* expression levels are positively correlated with BRAC purity and neutrophil infiltration levels [56–63]. In line with these results, another study reported that patients with mBC had higher levels of circulating VEGFA than patients without metastases [64]. VEGF can stimulate neutrophil migration through the activation of VEGFR1, [65] and can prevent dendritic cells from maturing, resulting in cytotoxic T cells' inactivation [66]. Tregs, tumor-associated macrophages, and myeloid-derived suppressor cells are all highly induced by VEGF, resulting in an immunosuppressive TME [67]. Furthermore, VEGF increases the expression of PD-1 on CD8+ CTLs and Tregs in a VEGFR2-dependent manner, [64] as well as the expression of Fas ligand, interleukin (IL)-10, and prostaglandin E3, leading to cytotoxic T cells' depletion [65]. Hence, VEGF-A can be used as a biomarker for immune-targeting therapy in breast cancer patients [66].

Histone deacetylase 1 (HDAC1) is overexpressed in breast cancer cells and human breast cancer tissues and can trigger the proliferation and migration of these cells via activation of Snail/IL-8 signals [41]. *HDAC1* suppression has been reported to reduce the invasion of breast cancer cells by inhibiting matrix metalloproteinase-9, [67] and to reduce PD-L1 and HLA-DR expression and Treg frequency in triple negative breast cancer [68]. In our study, there was a positive correlation between *HDAC1* expression levels and tumor purity, and CD8+ T cells', CD4+ T cells', neutrophils', and dendritic cells' infilitration levels.

HSP90α, encoded by *HSP90AA1*, is the stress-inducible isoform of HSP90. Previous studies have shown that high expression levels of HSP90 (HSP90α and HSP90β) increase the likelihood of recurrence and distant metastases in triple negative and ER+/HER2-breast cancer, and are associated with higher mortality [69]. Overexpression of HSP90 in human breast cancer cells has been linked to enhanced cell proliferation [42] and metastasis, [70] as well as to short OS and aggressive clinicopathological characteristics, such as high clinical stage, large tumors, and lymph node involvement [71]. Lin et al. reported that elevated *HSP90AB1* expression was linked to a better overall survival of ER- and Basal-like breast cancer patients [55]. However, we found that high *HSP90AB1* expression was associated with poor prognosis in BRCA patients. Additionally, the expression of *HSP90AA1* and *HSP90AB1* was positively correlated with tumor purity; and the expression of *HSP90AA1* was positively related to CD8+ T cells, macrophages, and neutrophils, but negatively correlated with CD4+ T cells. Further studies for exploring the infiltration of CD8+, macrophages, neutrophils, CD4+, and the effects of HNK on *HSP90AA1* and *HSP90AB1* are warranted.

CASP9 encodes caspase-9, an initiator of the intrinsic apoptosis pathway [79]. When the apoptosome, a multimolecular complex comprising cytochrome c and the apoptotic peptidase activating factor 1 (Apaf-1), is formed, it cleaves pro-caspase-9, forming caspase-9, triggering the caspase activation cascade by activating executor caspases, including caspase 3 and caspase 7 to cleave other cellular targets [80].

The aurora kinase family includes Aurora kinase B (AURKB), a mitotic serine/threonine protein kinase, and aurora kinase A (AURKA), which is a member of the Chromosomal Passenger Complex (CPC). The CPC plays a role in cell cycle progression and is a prognostic marker of

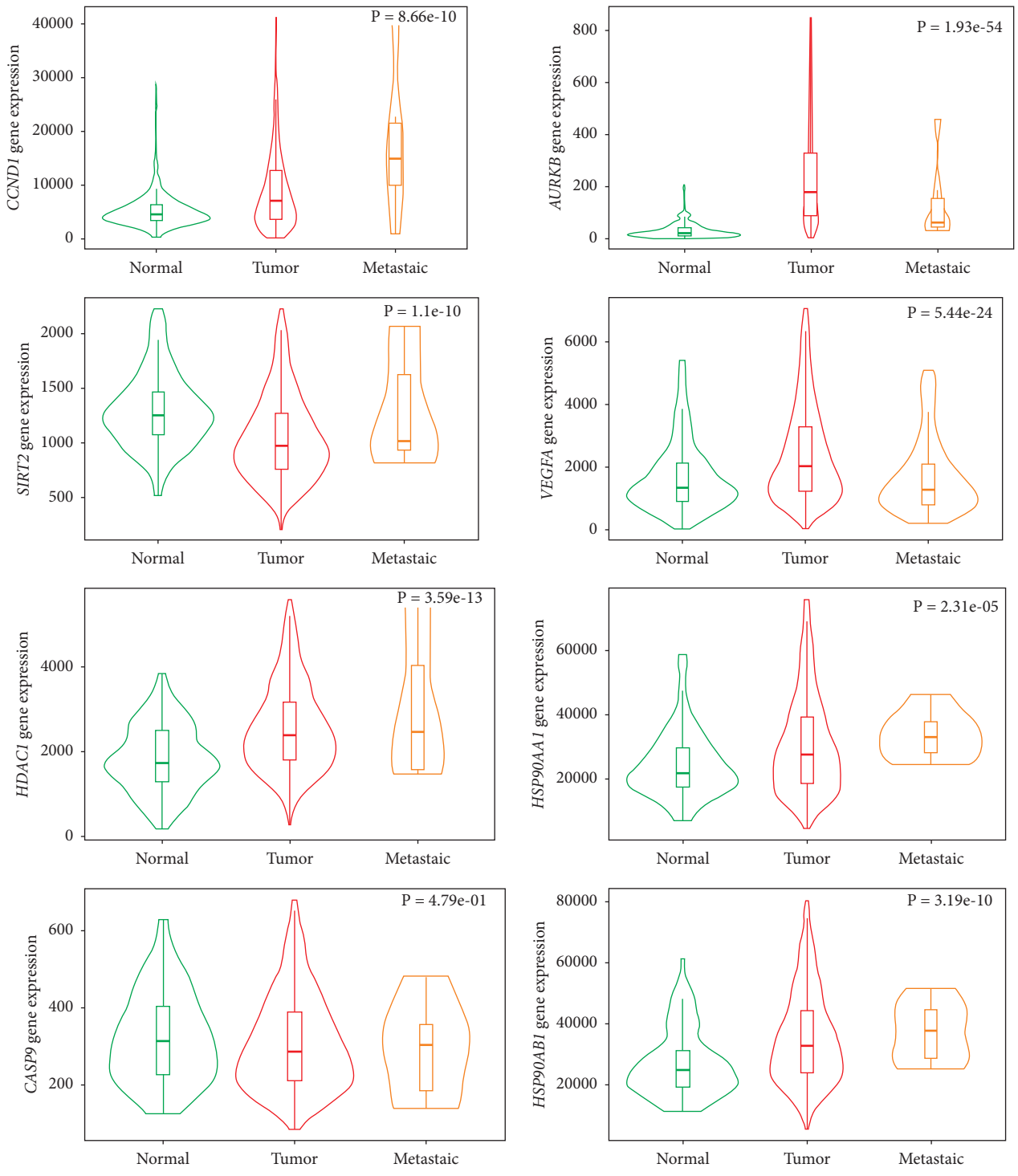

(a)

Figure 4: Continued.

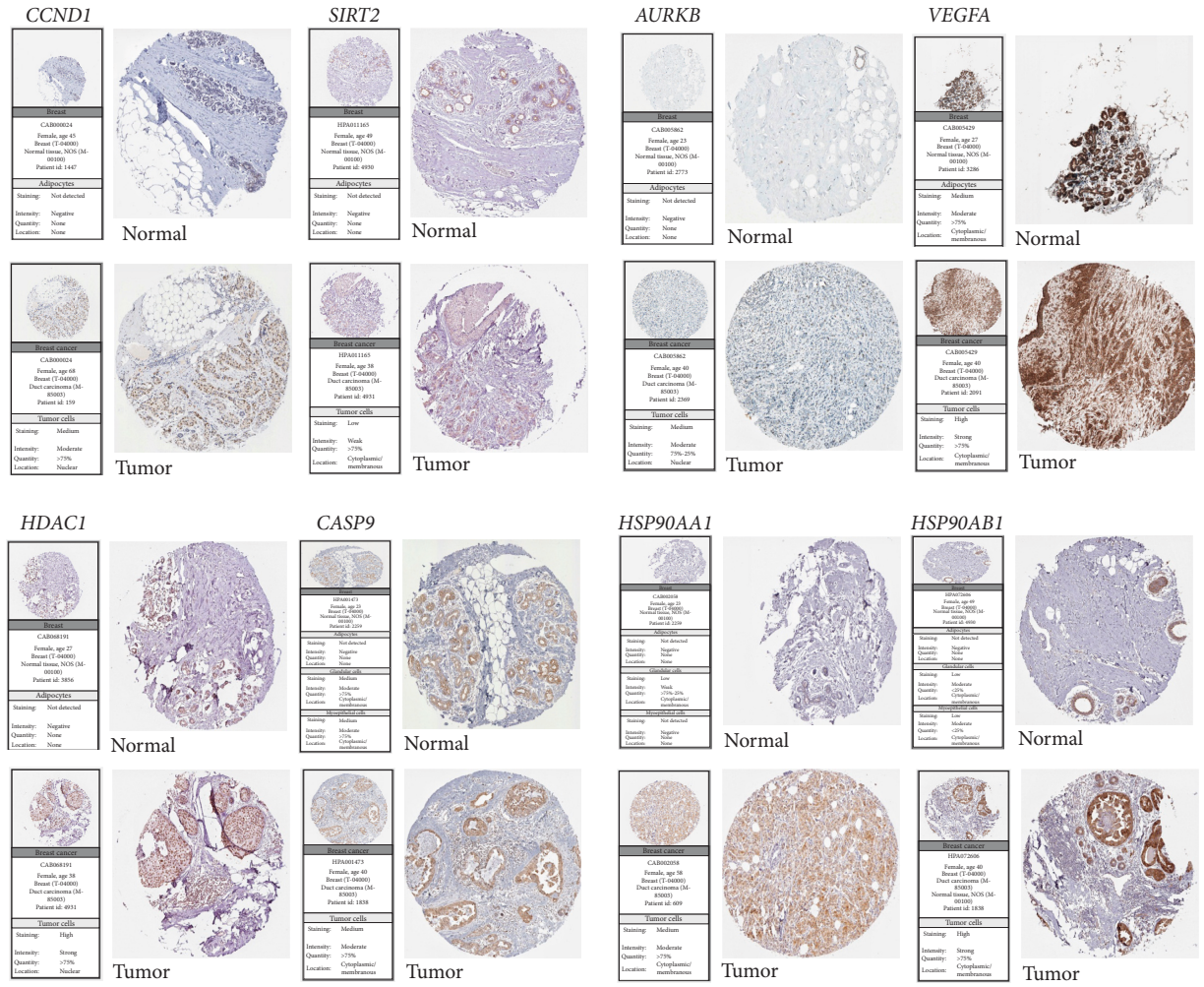

(b)

Figure 4: mRNA and the protein expression levels of *CCND1*, *SIRT2*, *AURKB*, *VEGFA*, *HDAC1*, *CASP9*, *HSP90AA1*, and *HSP90AB1*. (a) mRNA expression levels in the Cancer Genome Atlas (TCGA). (b) Protein expression levels in normal and tumor breast tissues retrieved from the Human Protein Atlas (HPA).

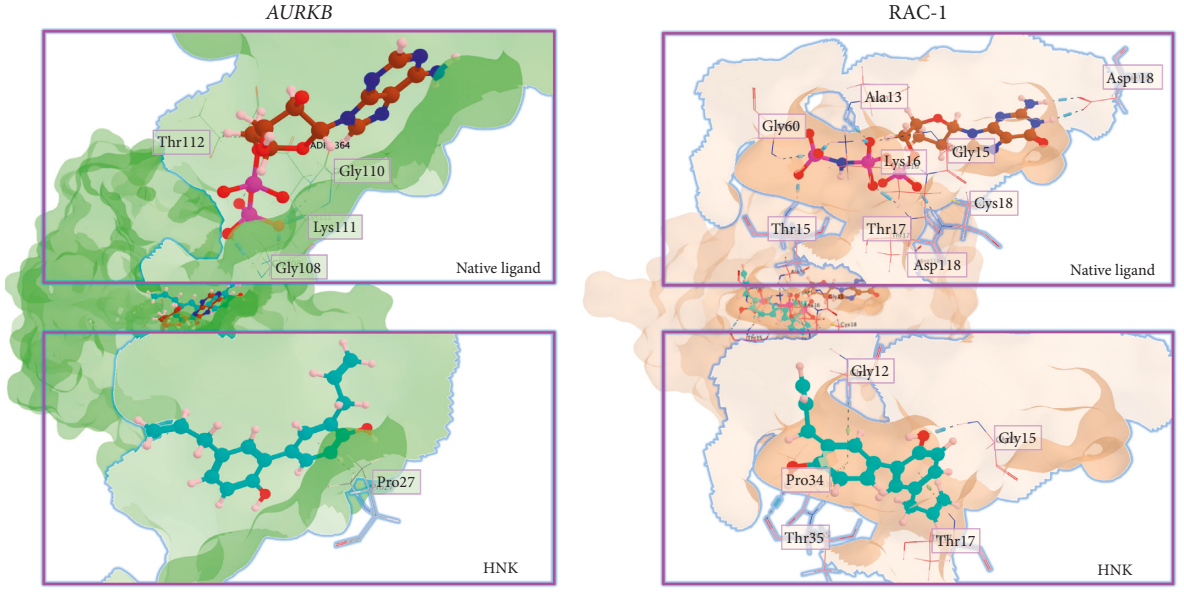

Figure 5: Visualization of molecular docking of honokiol (HNK) toward AURKB and RAC-1.

Table 4: Molecular docking results of honokiol (HNK) toward AURKB and RAC-1.

Protein, PDB ID	Native ligand						Honokiol					
	S	RMSD (Å)	LA	AA	BT	D	S	RMSD (Å)	LA	AA	BT	D
AURKB, PDB ID : 3ZCW	**−12.89**	1.39	O	Gly108	ScD	1.95	−8.68	1.10	C	Pro27	ArH	2.75
			O	Gly110	ScD	1.91						
			O	Lys111	ScD	2.11						
			O	Thr112	ScD	2.24						
			O	Ala13	ScD	2.20						
			O	**Gly15**	ScD	2.49						
RAC-1, PDB ID : 3TH5	**−21.38**	0.48	O	Lys16	ScD	1.73	−18.17	1.86	C	Gly12	ArH	4.01
			O	Lys16	ScD	1.95			O	**Gly15**	ScD	1.83
			O	**Thr17**	ScD	1.90			C	**Thr17**	ArH	3.35
			O	Cys18	ScD	1.79			C	Pro34	ArH	3.96
			O	**Thr35**	ScD	1.82			O	**Thr35**	ScA	2.14
			O	Gly60	ScD	2.37			C	**Thr35**	ArH	2.70
			H	Asp118	ScD	2.09						
			H	Asp118	ScD	2.13						

S: docking score, RMSD: root mean square deviation, LA: ligand atom, AA: amino acid, BT: binding type, D: distance, ScD: sidechain donor, ScA: sidechain acceptor, ArH: arene H, and BbD: backbone donor.

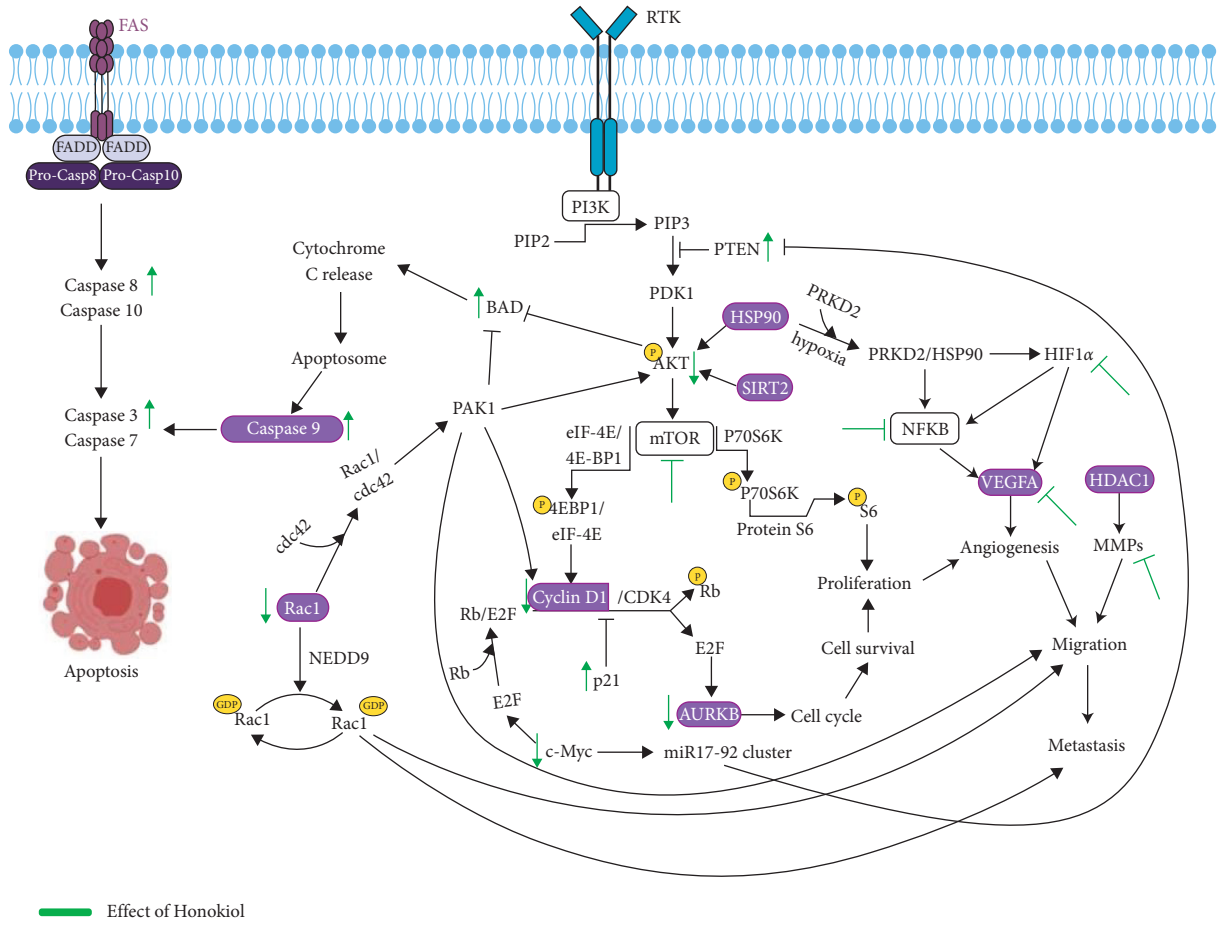

Figure 6: Proposed mechanism of honokiol (HNK) in mBCSCs (created with https://BioRender.com).

breast cancer arising from *BRCA2* mutation [81]. Deregulation of AURKB is observed in several tumors, and its overexpression is frequently linked to tumor cell invasion, metastasis, and drug resistance [82]. Hence, AURKB has emerged as an attractive drug target for the development of small-molecule inhibitors [83].

RAC1 and AURKB were selected for in-depth molecular docking analysis because they were connected to the PTTH-

mBCSCs-cell cycle axis. The Rho-GTPase family, including Rho, Rac1, and Cdc42, regulates the cytoskeleton [84] and thus modulates cell motility, migration, and invasion [85]. Rac-1/Cdc42 activation can induce cell growth by activating the PAK1/cyclin D1 pathway, or cell death by activating the PAK1/Akt/BAD pathway [86]. Rho has been suggested to be a potential therapeutic target, since Rho and *VEGFA* crosstalk leads to cancer progression and metastasis [87].

This study revealed the potential targets and molecular mechanisms of HNK on the cell cycle of mBCSCs (Figure 6). It is known that HNK exerts anticancer effects by suppressing angiogenesis, migration, invasion, and proliferation in a variety of cancer cell lines and tumor models [12]. HNK inhibits the cell cycle via the PI3K/Akt/mTOR pathway by upregulating PTEN and P21, and suppressing p-Akt, cyclin D/CDK4, c-Myc, Rac1, and *AURKB* [13, 14, 22, 71]. Angiogenesis is inhibited through the HIF1/NFkB pathway, which is activated under hypoxic conditions and blocks the release of VEGF. Immune infiltration analysis showed that HNK is correlated with *VEGFA* inhibition, suggesting HNK can effectively block VEGFR2. HNK was also found to reduce HIF-induced VEGFR/VEGF activation and inhibit matrix metalloproteinases activity and cell migration [88]. In addition, HNK can induce apoptosis through the upregulation of BAD, caspase-9, caspase-3, and caspase-8 [89]. In the tumor microenvironment, oncogenic drivers such as β-catenin, STAT3, PI3K/PTEN/AKT/mTOR, p53, NF-kB, and RAS/RAF/MAPK are activated to suppress the production of chemokines, reduce the recruitment of dendritic cells, macrophages, T cells, and NK cells to tumor sites, and to suppress the immune system of these immunocytes [90]. Furthermore, tumor-intrinsic signaling can cause tumor cells to express PD-L1, resulting in T cell dysfunction in the tumor microenvironment. This study highlights the potential of HNK as an immunotherapeutic agent for mBCSCs by modulating the tumor immune environment. However, the results of this study were obtained through bioinformatics studies; therefore, further in vitro, in vivo, and clinical trials are needed to validate the findings.

5. Conclusions

This study identified eight PTTHs consisting of *CCND1*, *SIRT2*, *AURKB*, *VEGFA*, *HDAC1*, *CASP9*, *HSP90AA1*, and *HSP90AB1*, which can inhibit the mBCSC-cell cycle axis. In addition, PTTHs may regulate the PI3K/Akt/mTOR and HIF1/NFkB pathways. This study is speeding up the development of HNK as anti-mBCSCs by targeting certain genes. However, this study have several limitations; for example, the targets of HNK are predicted from database. Other additional machine learning algorithm will provide more validated candidates of HNK targets. Another limitation of this study is that we used a bioinformatics approach; therefore, more needs to be explored further for validation and clarification in laboratory experiments.

Data Availability

The data generated or analyzed during this study are included within the article and its supplementary files.

Conflicts of Interest

The authors declare that they have no conflicts of interest.

Acknowledgments

The authors acknowledge Mrs. Ririn Widarti for her assistance with administrative support. This research was funded by the Directorate of Research, Universitas Gadjah Mada, through the Rekognisi Tugas Akhir program (SK Rektor UGM No. 1185/UN1.P.III/SK/HUKOR/2021).

Supplementary Materials

Supplementary Table 1. Differentially expressed genes (DEGs) in metastatic breast cancer stem cells (mBCSCs) from the GSE 151191 dataset. *Supplementary Table 2*. Honokiol (HNK)-mediated proteins (HMPs), as retrieved from Swiss target prediction, STITCH, canSAR Black, and SEA. *Supplementary Table 3*. KEGG pathway enrichment analysis of OGs from both HMP and DEGs. *Supplementary Figure 1*. Flowchart for the screening of datasets. (*Supplementary Materials*)

References

[1] WHO, "Cancer today. estimated number of incident cases Indonesia, females, all ages," 2020, https://gco.iarc.fr/today/home.

[2] K. D. Miller, L. Nogueira, A. B. Mariotto et al., "Cancer treatment and survivorship statistics, 2019," *CA: A Cancer Journal for Clinicians*, vol. 69, no. 5, pp. 363–385, 2019.

[3] M. A. Elbaiomy, T. Akl, N. Atwan, A. A. Elsayed, M. Elzaafarany, and S. Shamaa, "Clinical impact of breast cancer stem cells in metastatic breast cancer patients," *Journal of Oncology*, vol. 2020, Article ID 2561726, 8 pages, 2020.

[4] J. Zhao, "Cancer stem cells and chemoresistance: the smartest survives the raid," *Pharmacology & Therapeutics*, vol. 160, pp. 145–158, 2016.

[5] D. Raman, A. K. Tiwari, V. Tiriveedhi, and J. A. Rhoades, "Editorial: the role of breast cancer stem cells in clinical outcomes," *Frontiers in Oncology*, vol. 10, p. 299, 2020.

[6] A. A. Ross, "Minimal residual disease in solid tumor malignancies: a review," *Journal of Hematotherapy*, vol. 7, no. 1, pp. 9–18, 1998.

[7] M. De Angelis, F. Francescangeli, and A. Zeuner, "Breast cancer stem cells as drivers of tumor chemoresistance, dormancy and relapse: new challenges and therapeutic opportunities," *Cancers*, vol. 11, no. 10, p. 1569, 2019.

[8] M. Santisteban, J. M. Reiman, M. K. Asiedu et al., "Immune-induced epithelial to mesenchymal transition in vivo generates breast cancer stem cells," *Cancer Research*, vol. 69, no. 7, pp. 2887–2895, 2009.

[9] P. M. Aponte and A. Caicedo, "Stemness in cancer: stem cells, cancer stem cells, and their microenvironment," *Stem Cells International*, vol. 2017, Article ID 5619472, 17 pages, 2017.

[10] J. M. Pitt, A. Marabelle, A. Eggermont, J.-C. Soria, G. Kroemer, and L. Zitvogel, "Targeting the tumor microenvironment: removing obstruction to anticancer immune responses and immunotherapy," *Annals of Oncology*, vol. 27, no. 8, pp. 1482–1492, 2016.

[11] Y. C. Lo, T. Che-Ming, C. Chieh-Fu, C. Chien-Chih, and H. Chuang-Ye, "Magnolol and honokiol isolated from Magnolia officinalis protect rat heart mitochondria against lipid peroxidation," *Biochemical Pharmacology*, vol. 47, no. 3, pp. 549–553, 1994.

[12] S. Arora, S. Singh, G. A. Piazza, C. M. Contreras, J. Panyam, and A. P. Singh, "Honokiol: a novel natural agent for cancer prevention and therapy," *Current Molecular Medicine*, vol. 12, no. 10, pp. 1244–1252, 2012.

[13] I. Wolf, J. O'Kelly, N. Wakimoto et al., "Honokiol, a natural biphenyl, inhibits in vitro and in vivo growth of breast cancer through induction of apoptosis and cell cycle arrest," *International Journal of Oncology*, vol. 30, no. 6, pp. 1529–1537, 2007.

[14] E.-J. Park, H.-Y. Min, H.-J. Chung et al., "Down-regulation of c-Src/EGFR-mediated signaling activation is involved in the honokiol-induced cell cycle arrest and apoptosis in MDA-MB-231 human breast cancer cells," *Cancer Letters*, vol. 277, no. 2, pp. 133–140, 2009.

[15] J. Lee, J. Sul, J. Park, M. Lee, E. Cha, and Y. Ko, "Honokiol induces apoptosis and suppresses migration and invasion of ovarian carcinoma cells via AMPK/mTOR signaling pathway," *International Journal of Molecular Medicine*, vol. 43, no. 5, pp. 1969–1978, 2019.

[16] J. Wen, X. Wang, H. Pei et al., "Anti-psoriatic effects of Honokiol through the inhibition of NF-κB and VEGFR-2 in animal model of K14-VEGF transgenic mouse," *Journal of Pharmacological Sciences*, vol. 128, no. 3, pp. 116–124, 2015.

[17] S. Sengupta, A. Nagalingam, N. Muniraj et al., "Activation of tumor suppressor LKB1 by honokiol abrogates cancer stem-like phenotype in breast cancer via inhibition of oncogenic Stat3," *Oncogene*, vol. 36, no. 41, pp. 5709–5721, 2017.

[18] D. B. Avtanski, A. Nagalingam, P. Kuppusamy et al., "Honokiol abrogates leptin-induced tumor progression by inhibiting Wnt1-MTA1-β-catenin signaling axis in a microRNA-34a dependent manner," *Oncotarget*, vol. 6, no. 18, pp. 16396–16410, 2015.

[19] D. B. Avtanski, A. Nagalingam, M. Y. Bonner, J. L. Arbiser, N. K. Saxena, and D. Sharma, "Honokiol activates LKB1-miR-34a axis and antagonizes the oncogenic actions of leptin in breast cancer," *Oncotarget*, vol. 6, no. 30, pp. 29947–29962, 2015.

[20] N. Muniraj, S. Siddharth, M. Shriver et al., "Induction of STK11-dependent cytoprotective autophagy in breast cancer cells upon honokiol treatment," *Cell Death Discovery*, vol. 6, no. 1, pp. 81–15, 2020.

[21] W. Tian, Y. Deng, L. Li, H. He, J. Sun, and D. Xu, "Honokiol synergizes chemotherapy drugs in multidrug resistant breast cancer cells via enhanced apoptosis and additional programmed necrotic death," *International Journal of Oncology*, vol. 42, no. 2, pp. 721–732, 2013.

[22] C. Crane, A. Panner, R. O. Pieper, J. Arbiser, and A. T. Parsa, "Honokiol-mediated inhibition of PI3K/mTOR pathway," *Journal of Immunotherapy*, vol. 32, no. 6, pp. 585–592, 2009.

[23] M. Kuhn, C. von Mering, M. Campillos, L. J. Jensen, and P. Bork, "STITCH: interaction networks of chemicals and proteins," *Nucleic Acids Research*, vol. 36, pp. D684–D688, 2007.

[24] D. Gfeller, A. Grosdidier, M. Wirth, A. Daina, O. Michielin, and V. Zoete, "SwissTargetPrediction: a web server for target prediction of bioactive small molecules," *Nucleic Acids Research*, vol. 42, no. W1, pp. W32–W38, 2014.

[25] M. D. Halling-Brown, K. C. Bulusu, M. Patel, J. E. Tym, and B. Al-Lazikani, "CanSAR: an integrated cancer public translational research and drug discovery resource," *Nucleic Acids Research*, vol. 40, no. D1, pp. D947–D956, 2012.

[26] M. J. Keiser, V. Setola, J. J. Irwin et al., "Predicting new molecular targets for known drugs," *Nature*, vol. 462, no. 7270, pp. 175–181, 2009.

[27] H. Heberle, G. V. Meirelles, F. R. da Silva, G. P. Telles, and R. Minghim, "InteractiVenn: a web-based tool for the analysis of sets through Venn diagrams," *BMC Bioinformatics*, vol. 16, no. 1, p. 169, 2015.

[28] D. Szklarczyk, A. Franceschini, S. Wyder et al., "STRING v10: protein-protein interaction networks, integrated over the tree of life," *Nucleic Acids Research*, vol. 43, no. D1, pp. D447–D452, 2015.

[29] P. Shannon, A. Markiel, O. Ozier et al., "Cytoscape: a software environment for integrated models of biomolecular interaction networks," *Genome Research*, vol. 13, no. 11, pp. 2498–2504, 2003.

[30] C.-H. Chin, S.-H. Chen, H.-H. Wu, C.-W. Ho, M.-T. Ko, and C.-Y. Lin, "CytoHubba: identifying hub objects and sub-networks from complex interactome," *BMC Systems Biology*, vol. 8, no. S4, p. S11, 2014.

[31] W. da Huang W, B. T. Sherman, and R. A. Lempicki, "Bioinformatics enrichment tools: paths toward the comprehensive functional analysis of large gene lists," *Nucleic Acids Research*, vol. 37, no. 1, pp. 1–13, 2009.

[32] W. Wang, B. T. Vasaikar, R. A. Shi, R. A. Greer, and R. A. Zhang, "WebGestalt 2017: a more comprehensive, powerful, flexible and interactive gene set enrichment analysis toolkit," *Nucleic Acids Research*, vol. 45, no. 1, pp. W130–W137, 2017.

[33] E. Cerami, J. Gao, U. Dogrusoz et al., "The cBio cancer genomics portal: an open platform for exploring multidimensional cancer genomics data: figure 1," *Cancer Discovery*, vol. 2, no. 5, pp. 401–404, 2012.

[34] Z. Tang, C. Li, B. Kang, G. Gao, C. Li, and Z. Zhang, "GEPIA: a web server for cancer and normal gene expression profiling and interactive analyses," *Nucleic Acids Research*, vol. 45, no. W1, pp. W98–W102, 2017.

[35] T. Li, J. Fu, Z. Zeng et al., "TIMER2.0 for analysis of tumor-infiltrating immune cells," *Nucleic Acids Research*, vol. 48, no. W1, pp. W509–W514, 2020.

[36] Á Bartha and B. Győrffy, "TNMplot.com: a web tool for the comparison of gene expression in normal, tumor and metastatic tissues," *International Journal of Molecular Sciences*, vol. 22, no. 5, p. 2622, 2021.

[37] A. N. Tran, A. M. Dussaq, T. Kennell, C. D. Willey, and A. B. Hjelmeland, "HPAanalyze: an R package that facilitates the retrieval and analysis of the Human Protein Atlas data," *BMC Bioinformatics*, vol. 20, no. 1, p. 463, 2019.

[38] B. Zhao, A. Erwin, and B. Xue, "How many differentially expressed genes: a perspective from the comparison of genotypic and phenotypic distances," *Genomics*, vol. 110, no. 1, pp. 67–73, 2018.

[39] D. G. DeNardo, J. B. Barreto, P. Andreu et al., "$CD4^+$ T cells regulate pulmonary metastasis of mammary carcinomas by enhancing protumor properties of macrophages," *Cancer Cell*, vol. 16, no. 2, pp. 91–102, 2009.

[40] M. Binnewies, E. W. Roberts, K. Kersten et al., "Understanding the tumor immune microenvironment (TIME) for effective therapy," *Nature Medicine*, vol. 24, no. 5, pp. 541–550, 2018.

[41] M. F. Santolla and M. Maggiolini, "The FGF/FGFR system in breast cancer: oncogenic features and therapeutic perspectives," *Cancers*, vol. 12, no. 10, p. 3029, 2020.

[42] M. Zhang, S. Acklin, J. Gillenwater et al., "SIRT2 promotes murine melanoma progression through natural killer cell inhibition," *Scientific Reports*, vol. 11, no. 1, Article ID 12988, 2021.

[43] M. Malumbres and M. Barbacid, "To cycle or not to cycle: a critical decision in cancer," *Nature Reviews Cancer*, vol. 1, no. 3, pp. 222–231, 2001.

[44] E. A. Musgrove, C. E. Caldon, J. Barraclough, A. Stone, and R. L. Sutherland, "Cyclin D as a therapeutic target in cancer," *Nature Reviews Cancer*, vol. 11, no. 8, pp. 558–572, 2011.

[45] F. I. Montalto and F. De Amicis, "Cyclin D1 in cancer: a molecular connection for cell cycle control, adhesion and invasion in tumor and stroma," *Cells*, vol. 9, no. 12, p. 2648, 2020.

[46] T. G. Pestell, X. Jiao, M. Kumar et al., "Stromal cyclin D1 promotes heterotypic immune signaling and breast cancer growth," *Oncotarget*, vol. 8, no. 47, pp. 81754–81775, 2017.

[47] I. Karwaciak, A. Sałkowska, K. Karaś et al., "SIRT2 contributes to the resistance of melanoma cells to the multikinase inhibitor dasatinib," *Cancers*, vol. 11, no. 5, p. 673, 2019.

[48] V. Carafa, L. Altucci, and A. Nebbioso, "Dual tumor suppressor and tumor promoter action of sirtuins in determining malignant phenotype," *Frontiers in Pharmacology*, vol. 10, p. 38, 2019.

[49] L. Bosch-Presegue and A. Vaquero, "The dual role of sirtuins in cancer," *Genes & Cancer*, vol. 2, no. 6, pp. 648–662, 2011.

[50] L. Zhang, S. Kim, and X. Ren, "The clinical significance of *SIRT2* in malignancies: a tumor suppressor or an oncogene?" *Frontiers in Oncology*, vol. 10, p. 1721, 2020.

[51] C. Jiang, J. Liu, M. Guo et al., "The NAD-dependent deacetylase *SIRT2* regulates T cell differentiation involved in tumor immune response," *International Journal of Biological Sciences*, vol. 16, no. 15, pp. 3075–3084, 2020.

[52] A.-K. Olsson, A. Dimberg, J. Kreuger, and L. Claesson-Welsh, "VEGF receptor signalling ? in control of vascular function," *Nature Reviews Molecular Cell Biology*, vol. 7, no. 5, pp. 359–371, 2006.

[53] D. W. Leung, G. Cachianes, W.-J. Kuang, D. V. Goeddel, and N. Ferrara, "Vascular endothelial growth factor is a secreted angiogenic mitogen," *Science*, vol. 246, no. 4935, pp. 1306–1309, 1989.

[54] E. Tischer, D. Gospodarowicz, R. Mitchell et al., "Vascular endothelial growth factor: a new member of the platelet-derived growth factor gene family," *Biochemical and Biophysical Research Communications*, vol. 165, no. 3, pp. 1198–1206, 1989.

[55] D. J. Hicklin and L. M. Ellis, "Role of the vascular endothelial growth factor pathway in tumor growth and angiogenesis," *Journal of Clinical Oncology*, vol. 23, no. 5, pp. 1011–1027, 2005.

[56] B. Beck, G. Driessens, S. Goossens et al., "A vascular niche and a VEGF-Nrp1 loop regulate the initiation and stemness of skin tumours," *Nature*, vol. 478, no. 7369, pp. 399–403, 2011.

[57] D. Zhao, C. Pan, J. Sun et al., "VEGF drives cancer-initiating stem cells through VEGFR-2/Stat3 signaling to upregulate Myc and Sox2," *Oncogene*, vol. 34, no. 24, pp. 3107–3119, 2015.

[58] H. L. Goel, B. Pursell, C. Chang et al., "GLI1 regulates a novel neuropilin-2/$\alpha 6\beta 1$ integrin based autocrine pathway that contributes to breast cancer initiation," *EMBO Molecular Medicine*, vol. 5, no. 4, pp. 488–508, 2013.

[59] S. Bao, Q. Wu, S. Sathornsumetee et al., "Stem cell-like glioma cells promote tumor angiogenesis through vascular endothelial growth factor," *Cancer Research*, vol. 66, no. 16, pp. 7843–7848, 2006.

[60] P. Hamerlik, J. D. Lathia, R. Rasmussen et al., "Autocrine VEGF-VEGFR2-neuropilin-1 signaling promotes glioma stem-like cell viability and tumor growth," *Journal of Experimental Medicine*, vol. 209, no. 3, pp. 507–520, 2012.

[61] R. E. Bachelder, M. A. Wendt, and A. M. Mercurio, "Vascular endothelial growth factor promotes breast carcinoma invasion in an autocrine manner by regulating the chemokine receptor CXCR4," *Cancer Research*, vol. 62, no. 24, pp. 7203–7206, 2002.

[62] O. Gonzalez-Moreno, J. Lecanda, J. E. Green et al., "VEGF elicits epithelial-mesenchymal transition (EMT) in prostate intraepithelial neoplasia (PIN)-like cells via an autocrine loop," *Experimental Cell Research*, vol. 316, no. 4, pp. 554–567, 2010.

[63] L. S. Kim, S. Huang, W. Lu, D. Chelouche Lev, and J. E. Price, "Vascular endothelial growth factor expression promotes the growth of breast cancer brain metastases in nude mice," *Clinical & Experimental Metastasis*, vol. 21, no. 2, pp. 107–118, 2004.

[64] J. Adams, P. J. Carder, S. Downey et al., "Vascular endothelial growth factor (VEGF) in breast cancer: comparison of plasma, serum, and tissue VEGF and microvessel density and effects of tamoxifen," *Cancer Research*, vol. 60, no. 11, pp. 2898–2905, 2000.

[65] C. L. Roland, K. D. Lynn, J. E. Toombs, S. P. Dineen, D. G. Udugamasooriya, and R. A. Brekken, "Cytokine levels correlate with immune cell infiltration after anti-VEGF therapy in preclinical mouse models of breast cancer," *PLoS One*, vol. 4, no. 11, Article ID e7669, 2009.

[66] D. I. Gabrilovich, H. L. Chen, K. R. Girgis et al., "Production of vascular endothelial growth factor by human tumors inhibits the functional maturation of dendritic cells," *Nature Medicine*, vol. 2, no. 10, pp. 1096–1103, 1996.

[67] D. Lindau, P. Gielen, M. Kroesen, P. Wesseling, and G. J. Adema, "The immunosuppressive tumour network: myeloid-derived suppressor cells, regulatory T cells and natural killer T cells," *Immunology*, vol. 138, no. 2, pp. 105–115, 2013.

[68] T. Voron, O. Colussi, E. Marcheteau et al., "VEGF-A modulates expression of inhibitory checkpoints on CD8+ T cells in tumors," *Journal of Experimental Medicine*, vol. 212, no. 2, pp. 139–148, 2015.

[69] G. T. Motz, S. P. Santoro, L.-P. Wang et al., "Tumor endothelium fasL establishes a selective immune barrier promoting tolerance in tumors," *Nature Medicine*, vol. 20, no. 6, pp. 607–615, 2014.

[70] T. Fujii, T. Hirakata, S. Kurozumi et al., "VEGF-A is associated with the degree of TILs and PD-L1 expression in primary breast cancer," *In Vivo*, vol. 34, no. 5, pp. 2641–2646, 2020.

[71] Z. Tang, S. Ding, H. Huang et al., "*HDAC1* triggers the proliferation and migration of breast cancer cells via upregulation of interleukin-8," *Biological Chemistry*, vol. 398, no. 12, pp. 1347–1356, 2017.

[72] S. Y. Park, J. A. Jun, K. J. Jeong et al., "Histone deacetylases 1, 6 and 8 are critical for invasion in breast cancer," *Oncology Reports*, vol. 25, no. 6, pp. 1677–1681, 2011.

[73] M. Terranova-Barberio, S. Thomas, N. Ali et al., "HDAC inhibition potentiates immunotherapy in triple negative breast cancer," *Oncotarget*, vol. 8, no. 69, pp. 114156–114172, 2017.

[74] Q. Cheng, J. T. Chang, J. Geradts et al., "Amplification and high-level expression of heat shock protein 90 marks aggressive phenotypes of human epidermal growth factor receptor 2 negative breast cancer," *Breast Cancer Research*, vol. 14, no. 2, pp. R62–R15, 2012.

[75] M. Yano, Z. Naito, M. Yokoyama et al., "Expression of hsp90 and cyclin D1 in human breast cancer," *Cancer Letters*, vol. 137, no. 1, pp. 45–51, 1999.

[76] H. Liu, Z. Zhang, Y. Huang et al., "Plasma *HSP90AA1* predicts the risk of breast cancer onset and distant metastasis," *Frontiers in Cell and Developmental Biology*, vol. 9, Article ID 639596, 2021.

[77] M. Klimczak, P. Biecek, A. Zylicz, and M. Zylicz, "Heat shock proteins create a signature to predict the clinical outcome in breast cancer," *Scientific Reports*, vol. 9, no. 1, p. 7507, 2019.

[78] T. Lin, Y. Qiu, W. Peng, and L. Peng, "Heat shock protein 90 family isoforms as prognostic biomarkers and their correlations with immune infiltration in breast cancer," *BioMed Research International*, vol. 2020, Article ID 2148253, 15 pages, 2020.

[79] H. Liu, C. Zang, A. Emde et al., "Anti-tumor effect of honokiol alone and in combination with other anti-cancer agents in breast cancer," *European Journal of Pharmacology*, vol. 591, no. 1-3, pp. 43–51, 2008.

[80] D. B. Avtanski, A. Nagalingam, M. Y. Bonner, J. L. Arbiser, N. K. Saxena, and D. Sharma, "Honokiol inhibits epithelial-mesenchymal transition in breast cancer cells by targeting signal transducer and activator of transcription 3/Zeb1/E-cadherin axis," *Molecular Oncology*, vol. 8, no. 3, pp. 565–580, 2014.

[81] A. Tang, K. Gao, L. Chu, R. Zhang, J. Yang, and J. Zheng, "Aurora kinases: novel therapy targets in cancers," *Oncotarget*, vol. 8, no. 14, pp. 23937–23954, 2017.

[82] J. Bertran-Alamillo, V. Cattan, M. Schoumacher et al., "AURKB as a target in non-small cell lung cancer with acquired resistance to anti-EGFR therapy," *Nature Communications*, vol. 10, no. 1, pp. 1812–1814, 2019.

[83] A. Ahmed, A. Shamsi, T. Mohammad, G. M. Hasan, A. Islam, and M. I. Hassan, "Aurora B kinase: a potential drug target for cancer therapy," *Journal of Cancer Research and Clinical Oncology*, vol. 147, no. 8, pp. 2187–2198, 2021.

[84] A. J. Ridley, H. F. Paterson, C. L. Johnston, D. Diekmann, and A. Hall, "The small GTP-binding protein rac regulates growth factor-induced membrane ruffling," *Cell*, vol. 70, no. 3, pp. 401–410, 1992.

[85] C. T. Mierke, S. Puder, C. Aermes, T. Fischer, and T. Kunschmann, "Effect of PAK inhibition on cell mechanics depends on Rac1," *Frontiers in Cell and Developmental Biology*, vol. 8, p. 13, 2020.

[86] K. Zins, T. Lucas, P. Reichl, D. Abraham, and S. Aharinejad, "A rac1/cdc42 GTPase-specific small molecule inhibitor suppresses growth of primary human prostate cancer xenografts and prolongs survival in mice," *PLoS One*, vol. 8, no. 9, Article ID e74924, 2013.

[87] N. El Baba, M. Farran, E. A. Khalil, L. Jaafar, I. Fakhoury, and M. El-Sibai, "The role of Rho GTPases in VEGF signaling in cancer cells," *Analytical Cellular Pathology*, vol. 2020, Article ID 2097214, 11 pages, 2020.

[88] C. P. Ong, W. L. Lee, Y. Q. Tang, and W. H. Yap, "Honokiol: a review of its anticancer potential and mechanisms," *Cancers*, vol. 12, no. 1, p. 48, 2019.

[89] H. Xu, W. Tang, G. Du, and N. Kokudo, "Targeting apoptosis pathways in cancer with magnolol and honokiol, bioactive constituents of the bark of Magnolia officinalis," *Drug Discoveries & Therapeutics*, vol. 5, no. 5, pp. 202–210, 2011.

[90] K. Stankov, S. Popovic, and M. Mikov, "C-KIT signaling in cancer treatment," *Current Pharmaceutical Design*, vol. 20, no. 17, pp. 2849–2880, 2014.